PAPER

Highly stable cesium lead iodide perovskite quantum dot light-emitting diodes

To cite this article: Chen Zou *et al* 2017 *Nanotechnology* **28** 455201

View the article online for updates and enhancements.

Related content

Highly stable cesium lead iodide perovskite quantum dot light-emitting diodes

Chen Zou[1,4] , Chun-Ying Huang[1,2,4], Erin M Sanehira[1,3], Joseph M Luther[3] and Lih Y Lin[1]

[1] Department of Electrical Engineering, University of Washington, Seattle, WA 98195, United States of America
[2] Department of Applied Materials and Optoelectronic Engineering, National Chi Nan University, NanTou 54561, Taiwan
[3] Chemical and Materials Science, National Renewable Energy Laboratory (NREL), Golden, CO 80401, United States of America

E-mail: lylin@uw.edu

Abstract

Recently, all-inorganic perovskites such as $CsPbBr_3$ and $CsPbI_3$, have emerged as promising materials for light-emitting applications. While encouraging performance has been demonstrated, the stability issue of the red-emitting $CsPbI_3$ is still a major concern due to its small tolerance factor. Here we report a highly stable $CsPbI_3$ quantum dot (QD) light-emitting diode (LED) with red emission fabricated using an improved purification approach. The device achieved decent external quantum efficiency (EQE) of 0.21% at a bias of 6 V and outstanding operational stability, with a L_{70} lifetime (EL intensity decreases to 70% of starting value) of 16 h and 1.5 h under a constant driving voltage of 5 V and 6 V (maximum EQE operation) respectively. Furthermore, the device can work under a higher voltage of 7 V (maximum luminance operation) and retain 50% of its initial EL intensity after 500 s. These findings demonstrate the promise of $CsPbI_3$ QDs for stable red LEDs, and suggest the feasibility for electrically pumped perovskite lasers with further device optimizations.

Supplementary material for this article is available online

Keywords: stability, perovskite quantum dot, LED, red emission

(Some figures may appear in colour only in the online journal)

1. Introduction

Recent years have been marked with increased attention to achievement by solution-processed halide perovskite materials in the field of light-emitting diodes (LEDs) [1–4]. Most of the prior work use organic–inorganic hybrid perovskites, such as $CH_3NH_3PbBr_3$ ($MAPbBr_3$) as active layers [5–7]. Despite the demonstrated strong photoluminescence quantum yields (PLQY), the stability issue of $MAPbBr_3$ remains a critical challenge for further development and commercialization of perovskite-based LEDs. More recently, a growing number of research studies have been devoted to all-inorganic perovskites, such as cesium lead bromide ($CsPbBr_3$), which exhibit higher thermal stability and outstanding optical properties, especially their high PLQY [8, 9]. However, cubic phase $CsPbI_3$ bulk films, which is required to generate red light, are still only stable at high temperature above 300 °C, which is not desirable for practical applications. Our previous work has shown quantum dot (QD) surfaces can be used to stabilize cubic phase $CsPbI_3$ at room temperature [10]. Furthermore, QD structure is desirable for LED applications due to the added ability of precise control over the emission wavelength with a narrow emission spectrum and strong quantum confinement effect. As a result, all-inorganic perovskite QDs have been pursued as LED materials and have been demonstrated with higher thermal stability compared to

the organic cation-based perovskites [11–16]. Although some stability tests have been performed on the all-inorganic perovskite QD-based LEDs, there is limited study on the mechanisms of device degradation in the literature, which is required before this research field can be further developed for practical applications.

To generate high-power white light for illumination, one of the effective approaches is to use individual LEDs that emit three primary colors and then mix all the colors to form white light. All-inorganic perovskite LEDs based on $CsPbBr_3$ QDs have been investigated as a green light source, and a peak external quantum efficiency (EQE) exceeding 8.7% has recently been demonstrated [17]. To achieve red-emitting perovskite LEDs which is indispensable for white light generation, $CsPbI_3$ QDs readily emit in the proper wavelength range. However, reported research results on $CsPbI_3$ QD LEDs are still scarce at present, with electroluminescence from $CsPbI_3$ QDs reported recently [10, 11, 18, 19]. The underlying reason may be attributed to the small tolerance factor of $CsPbI_3$ QDs [20]. Goldschmidt's tolerance factor is an indicator for the stability and distortion of crystal structures [21], which accounts for the relative size of the constituent ions. Yakunin *et al* have demonstrated red LEDs fabricated with $FAPbI_3$ and $Cs_{0.9}FA_{0.1}PbI_3$ QDs with impressive colloidal stability [22], however, little is known about the operational stability of these red-emitting perovskite QD LEDs thus far. A novel purification method has been employed in our previous work for retaining the phase stability of the $CsPbI_3$ QDs [10]. In this study, we show that red-emitting LEDs consist of the above-mentioned all-inorganic $CsPbI_3$ QDs can achieve outstanding operational stability with a maximum EQE of 0.21%. Our LEDs achieve a high L_{70} lifetime over 16 h under a constant applied voltage of 5 V ($J = 23\,mA\,cm^{-2}$), the highest reported result for iodide-based perovskite LEDs so far to the best of our knowledge. At the same time, a decent peak EQE of 0.21% is obtained, which is comparable with other all-inorganic perovskite QD LEDs (see supplementary table S1 available online at stacks. iop.org/NANO/28/455201/mmedia in supporting information). Red emission which hits the red corner of Commission Internationale de l'Eclairage (CIE) chromaticity diagram also has been observed, enabling excellent display and white perovskite LED technology.

2. Experimental details

The fabrication method of $CsPbI_3$ QDs can be found in our previous report [10]. In general, methyl acetate (MeOAc) was added into the crude $CsPbI_3$ QD solution to wash and isolate QDs, the purified QDs were dispersed in hexane or octane. The formation of α-$CsPbI_3$ QDs are phase-stable for months in ambient. Recently, Zeng *et al* also reported the different performances of perovskite QDs by using different solvents for purification process [23]. The octane and hexane are usually used to disperse perovskite QDs since they have the similar polarity to that of the surface ligands (oleic acid and oleylamine). Given the ionicity of perovskites and the ionic

binding of the ligands, the solvents with high polarity like DMF and DMSO could completely dissolve the ionic perovskite. Therefore, the non-solvents with low polarity are preferred for purification process. Compared to 1-butanol, acetone, ethyl acetate, MeOAc was tested to be able to successfully extract the stable $CsPbI_3$ QDs with cubic phase. Other solvents destabilized QDs and resulted in pale yellow and PL inactive solution after a short time storage.

Material properties of the $CsPbI_3$ QDs were characterized first. UV–Visible absorption spectra of $CsPbI_3$ thin films were measured by Varian Cary 5000 UV–vis–NIR Spectrophotometer. Steady-state PL spectra were obtained using a spectrofluorometer (Fluorolog FL-3, Jobin Yvon Horiba) with xenon short arc lamp as the light source. Transient PL lifetime data were acquired using a time-correlated single-photon counting system (FluoTime 100, PicoQuant) with a pulse laser excitation source (470 nm, 60 ps, 40 MHz) at a low pump intensity.

The $CsPbI_3$ QD LED has a device structure with the following layers in order: indium tin oxide (ITO) coated glass, PEDOT:PSS (20 nm), $CsPbI_3$ QDs (~70 nm), TPBI (35 nm), LiF (1 nm)/Al (150 nm). Prepatterned ITO-coated glass substrates were first cleaned by sonication in detergent water, isopropyl alcohol and DI water sequentially for 30 min, followed by ozone plasma treatment for 15 min. The PEDOT: PSS solution was filtered by 0.45 um nylon syringe filters and spin-coated onto prepatterned ITO substrates at 4000 rpm for 30 s, followed by annealing on a hot plate at 140 °C for 15 min. Next, the $CsPbI_3$ QD solution was spin-coated at 1000 rpm for 45 s two times to obtain a continuous and smooth film. The as-coated substrates were then transferred into a N_2-filled glovebox. Finally, TPBI (35 nm), LiF (1 nm), and Al (150 nm) layers were deposited sequentially by thermal evaporation through shadow masks at the rate of 1.0, 0.1 and 2 Å s^{-1} respectively. The device area was 0.5 cm^2 as defined by the intersection area between the bottom ITO and top Al electrodes.

To evaluate the device performance, we carried out various characterizations on the devices in ambient conditions under room temperature with lab humidity of 65%. The EL spectra, CIE color coordinates and luminance (L)–current density (J)–voltages (V) characteristics were collected using a computer-controlled system incorporating a Keithley 2400 source meter and a Konica Minolta CS-2000 spectroradiometer. A calibrated Newport 818-UV Si photodetector (active area: 1 cm^2) was centered above one LED pixel at a fixed distance (2 cm) to measure the emitted front-face power output through the ITO substrate. Lambertian profile was used for calculating the EQE, which can be expressed as the ratio of the number of output photons to that of injected electrons [24]:

$$EQE = \frac{N_{photon}}{I/e} * \frac{a^2 + L^2}{a^2},$$

where N_{photon} is the number of emitted photons collected by the photodetector (calculated from the measured power and the corresponding EL spectrum), and I is the injection current. L is the distance between the light-emitting pixel and the
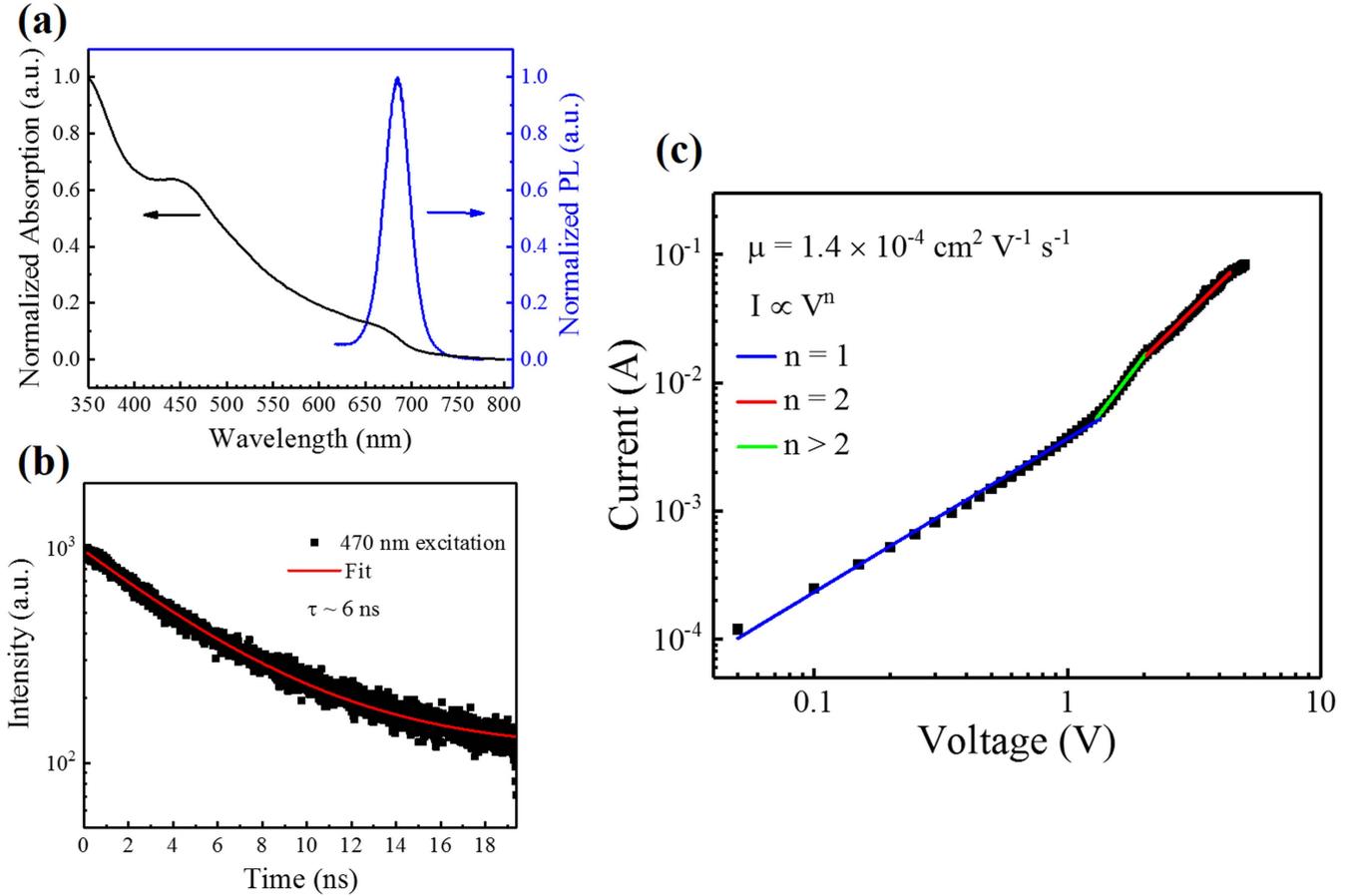
Figure 1. Characterizations of the CsPbI$_3$ QD film. (a) UV–Visible absorption and PL spectra. (b) Transient PL measurement. A lifetime of 6 ns was obtained from fitting the data. (c) *I–V* measurement of a hole-only device in the dark condition for extracting the mobility in the CsPbI$_3$ QD film using a space charge-limited current method.

photodetector, while *a* is the diameter of the photodetector active area.

3. Results and discussion

The UV–Visible absorption and PL spectra of the as-prepared CsPbI$_3$ QD film are shown in figure 1(a). We can observe a PL peak located at 685 nm. The absorption edge is also near 685 nm. We measured the absorption curves after 0, 5, and 10 d storage, and discovered an encouraging result that the absorption property of the material does not change significantly (see supplementary figure S1). Figure 1(b) shows the transient PL decay trace. A PL lifetime of ∼6 ns was extracted by fitting the data using a single-exponential decay model [18]. The charge mobility in the CsPbI$_3$ QD films can be measured using a space charge-limited current method [25–27]. Hole-only devices were fabricated using the structure ITO/PEDOT:PSS/CsPbI$_3$/Au, the energy level alignment makes the whole device only transport holes. Figure 1(c) shows the current dependence on voltage in dark condition. At first, the current shows linear dependence, which indicates an ohmic characteristic. The *I–V* curve shows a different pattern identified by the dramatic increase of the

current at 1.2 V, indicating the beginning of a trap-filling process. After the traps are completely filled, the device reaches the child region [27]. The dark current shows quadratic dependence on voltage (*I–V*^{2}) in this region. Furthermore, the dark current can be fitted by the Mott–Gurney law:

$$J_d = \frac{9\varepsilon\varepsilon_0\mu V^2}{8L^3},$$

where *V* is the applied voltage, J_d is the current density, ε (28) is the relative dielectric constant for CsPbI$_3$ QDs. *L* is the thickness of the CsPbI$_3$ QD film, which is estimated to be ∼100 nm from the scanning electron micrograph (SEM) image (see supporting information). From here, we can extract the mobility (μ) of our CsPbI$_3$ QDs to be 1.4×10^{-4} cm^2 V^{-1} s^{-1}, which is comparable to the reported mobility of 10^{-4} cm^2 V^{-1} s^{-1} in MAPbI$_3$ thin films [28] and other inorganic QDs like PbSe [29].

A schematic device structure is shown in figure 2(a), and the corresponding SEM cross-section image of the as-fabricated LED device is shown in figure 2(b). All device layers can be clearly identified. The flat-band energy diagram of the device is illustrated in figure 2(c), in which TPBI and PEDOT:PSS are employed as electron and hole transport layer, respectively [30]. On the other hand, they also block
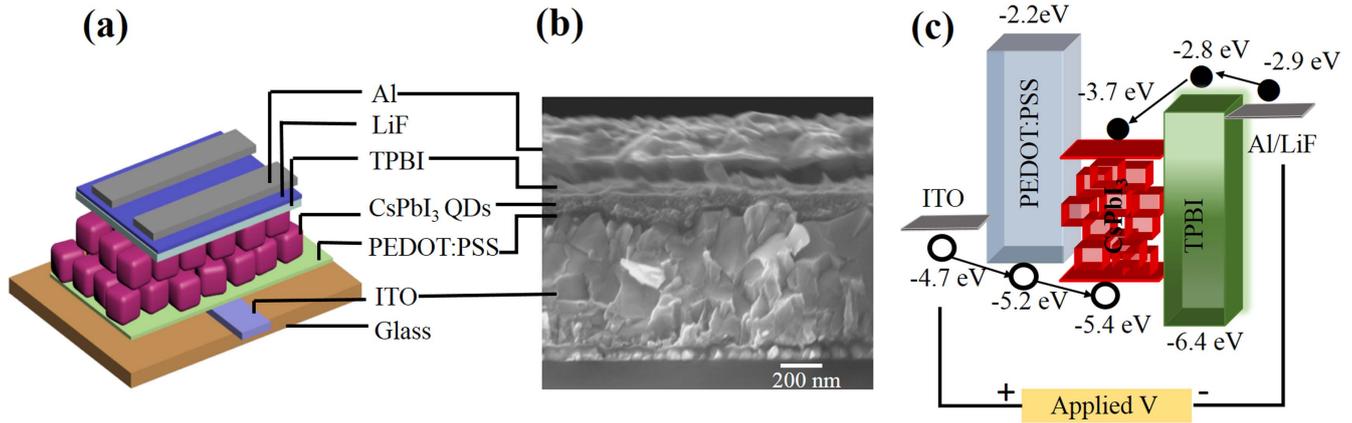
Figure 2. (a) Schematic diagram of the CsPbI$_3$ QD LED device structure. (b) The cross-section view SEM image of the fabricated device. (c) Energy band diagram of the LED device.
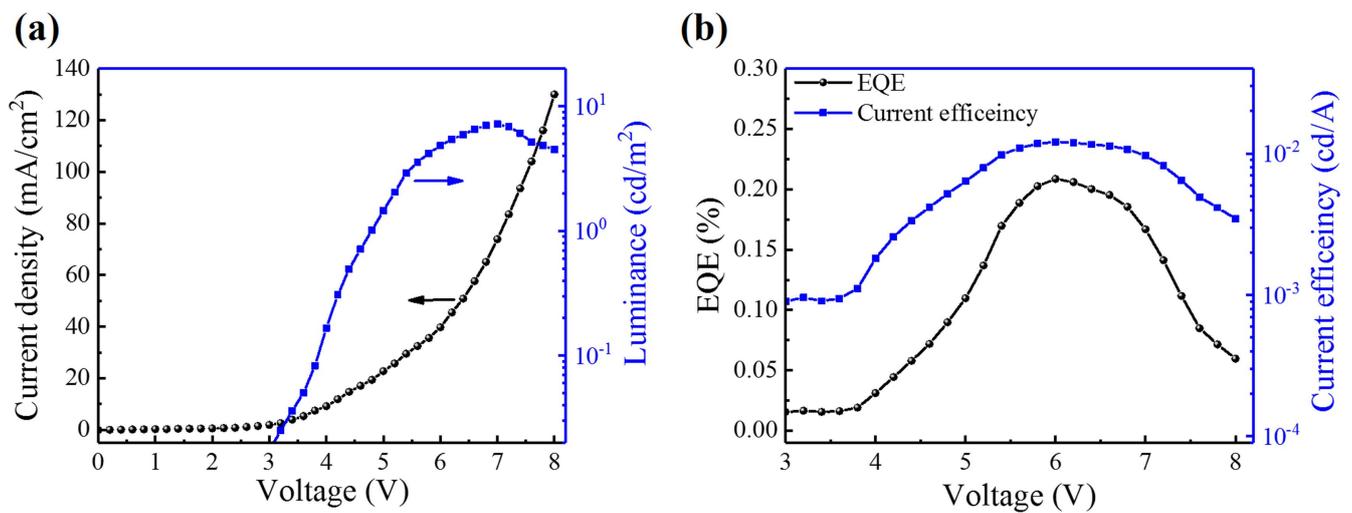
Figure 3. (a) Current density and luminance versus voltage, and (b) external quantum efficiency and current efficiency versus voltage for the CsPbI$_3$ QD LEDs.

holes and electrons respectively due to the appropriate HUMO and LOMO values, which facilitates the recombination of electro–hole pairs in the perovskite active layer.

The *L–J–V* characteristics of the device are presented in figure 3(a). The CsPbI$_3$ QD LED shows a clear diode characteristic with a low turn-on voltage V_{on} of 3 V. The luminance achieves a maximum value of 7.2 cd m^{-2} under a bias voltage of 7 V. The current efficiency and EQE as a function of the applied voltage in logarithmic and linear scale for the CsPbI$_3$ QD LED are shown in figure 3(b). A maximum current efficiency of 0.012 cd A^{-1} and EQE of 0.21% are observed at an applied bias of 6 V. The EQE can be further increased by enhancing the PLQY and conductivity of CsPbI$_3$ QD thin films in addition to better device design to minimize the energy barriers at all interfaces [14]. We also found that the active perovskite layer thickness affected EQE and device performance substantially. We spin-coated CsPbI$_3$ QDs with different spin parameters to change the active layer thickness. A maximum EQE was achieved by a two-cycle spin coating process, which resulted in an approximately 70 nm thick active layer (see supporting information).

Figure 4(a) presents the EL spectra of the CsPbI$_3$ QD LED under different applied biases. As the applied voltage increases, a narrow EL peak at 693 nm starts to emerge (FWHM linewidth $\Delta\lambda \sim 32$ nm). It should be noted that there are no notable parasitic emissions from the charge transport layers and the shape of the EL spectrum does not change at different applied voltages. These observations indicate that carriers are well confined in the perovskite QD layer and the recombination zone does not change in response to different applied voltages [3]. The inset of figure 4(a) shows the photograph of a bright and uniform red light from our CsPbI$_3$ QD LED in operation. The EL corresponds to the CIE color coordinates of (0.70, 0.26) at 5 V, which is on the red corner of the CIE color diagram, as shown in figure 4(b).

To further the advancement of perovskite materials for LED applications, understanding the device stability behavior under varying driving voltages is required. The operating lifetime is typically tested for the purpose of determining the resistance of materials under electrical and thermal stress. LED lifetime is measured by how the intensity of emitted light diminishes over time. According to IES TM21 standard
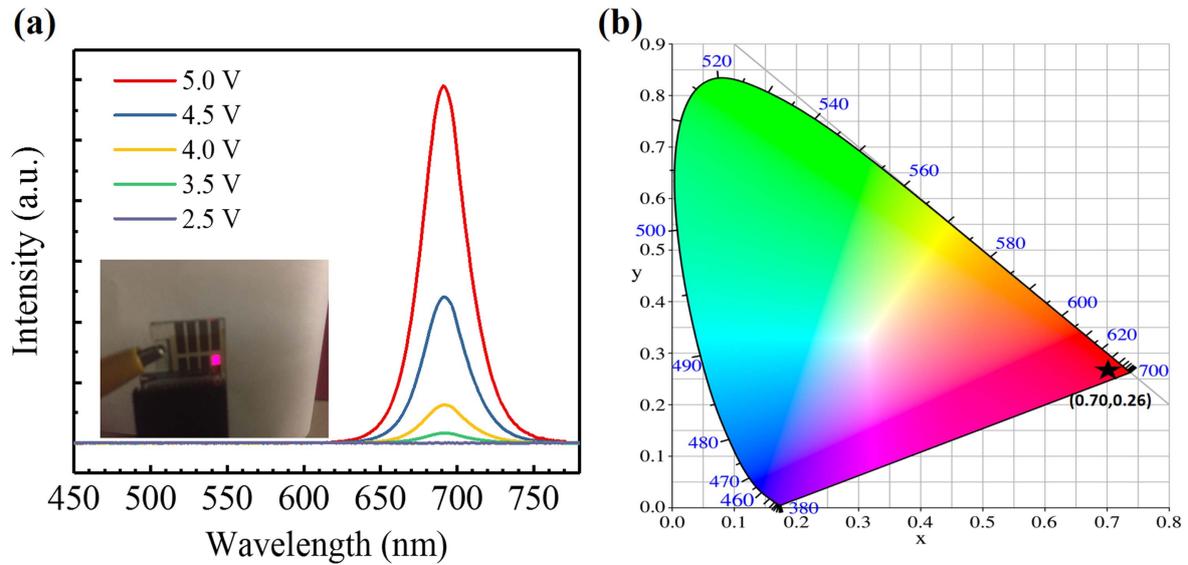
Figure 4. (a) EL spectra under different applied voltages. Inset: Photograph of the device in operation, showing red emission. (b) CIE coordinates of the emitted light from the CsPbI$_3$ QD LED.
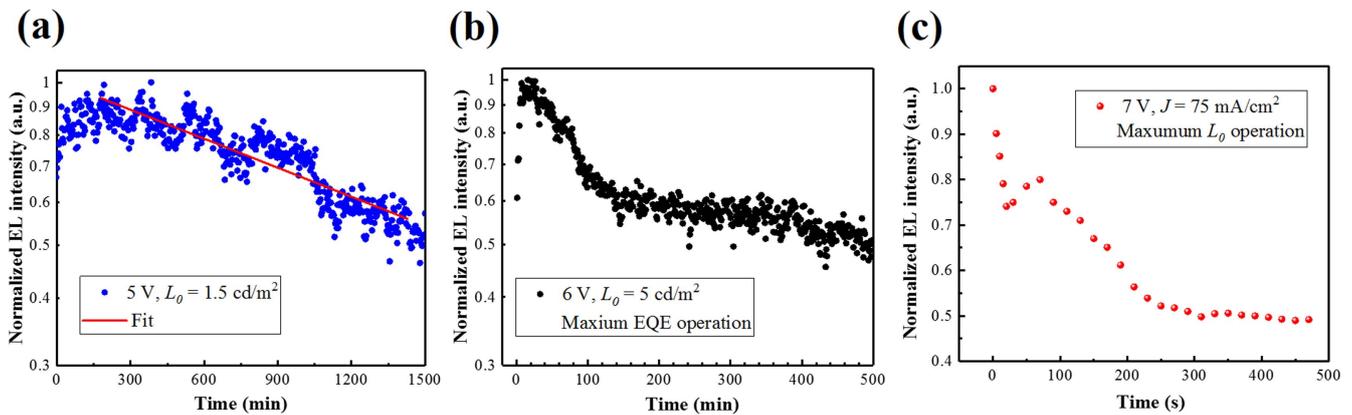
Figure 5. Stability characterizations of the device under (a) low bias of 5 V, (b) 6 V bias where maximum EQE is achieved, and (c) high bias and current injection condition (7 V, $J = 75$ mA cm^{-2}), where maximum luminance is reached. (a) and (b) are in logarithmic scale and (c) is in linear scale. The measurements were performed at room temperature under ambient conditions.

criterion, we define the time it takes for the EL intensity decreasing to 70% of the initial intensity as L_{70} lifetime (T_{70}). To evaluate the stability of the CsPbI$_3$ QD LEDs under different driving conditions, we applied different voltages to find the correlation between output EL and lifetime. The normalized EL intensity versus time under a constant applied bias of 5 V was recorded and presented in logarithmic scale in figure 5(a). The corresponding luminance at the starting point is about 1.5 cd m^{-2}. The EL intensity slightly increases during the first 3 h and then decreases steadily. The EL decay process can be fit well by a single-exponential decay model of $I = 0.92e^{-t/22} + 0.06$. The increase at the beginning may be attributed to an annealing effect on the perovskite QD film and/or improved interface contact caused by joule heating. During the operation of the fabricated LED, no evident changes in the peak position and shape of the EL spectra were observed. The device under the low applied bias of 5 V exhibits very high stability ($T_{70} \sim 16$ h). This is somewhat unexpected as the common belief is that the iodide ions would

result in perovskite QDs with low stability due to their metastable state in the cubic phase [16, 31]. We attribute this to the process of purification using MeOAc, which results in stable CsPbI$_3$ QDs in the cubic phase [10], and thus the long lifetime of our CsPbI$_3$ QD LEDs. More importantly, we found that such an EL decay is a temporary behavior, and the EL intensity could recover to its original status after a short relax time. This finding demonstrates that the treated CsPbI$_3$ QDs are thermally stable and will not decompose under such an applied bias and corresponding injection current ($J = 23$ mA cm^{-2}). The temperature of device increases inevitably during the stability test, which would increase nonradiative recombination rate and leads to the EL decay. To further investigate the device stability, a harsher condition with an applied bias of 6 V was used, where the device worked with the maximum EQE. The result is shown in figure 5(b). The corresponding luminance at the starting point is about 5 cd m^{-2}. In this case the output EL intensity from the light-emitting pixel also increases at the first 15 min. For

the EL intensity decay process, it is observed that there are fast and slow decay components, which is due to the high injection current at first and the device degrades very fast as a result. In this case, L_{70} lifetime is estimated to be 1.5 h. As shown in figure 5(c), under higher applied voltage of 7 V ($J = 75 \, \mathrm{mA \, cm^{-2}}$, maximum luminance operation), the device degrades more rapidly and retains 50% of its initial EL intensity after 500 s. Specifically, the EL intensity drops dramatically to 75% of initial value (L_0) at the first few seconds since the device is not able to stand such high current density. Then the device performs similarly to that in the low applied voltage condition. The perovskite QDs usually have lower mobility and thermal conductivity because of the insulating surface ligands and poor transport between QDs [32], thus they typically have bad thermal stability under high injection current. However, our CsPbI$_3$ QD LED device could still tolerate such a high injection current density for 500 s, which indicates that our CsPbI$_3$ QDs have good thermal stability. Our results under both low and high injection conditions compare favorably with reported results from literature for perovskite LEDs [14, 15, 33] (see supplementary table S1 for complete comparison). These findings provide insight for the feasibility of electrically pumped perovskite lasers which need high injection current density to enable population inversion [34]. The operational device stability under high current injection can be further optimized and improved by using thermally stable carrier transport layers, such as inorganic materials which usually generate less resistive heating and have better thermal stability [35].

4. Conclusion

In conclusion, we fabricated CsPbI$_3$ QD LEDs by adopting a novel purification route that enabled the QDs to retain the phase stability under current injection. Various device performance including EL spectra, CIE coordinates, L–J–V characteristics, luminance and EQE were characterized. We also performed stability measurements. Our devices achieved 16 h L_{70} lifetime under the applied voltage of 5 V. To the best of our knowledge this is the highest stability among iodide-based perovskite LEDs reported so far. The device also showed reliable performance operating at 6 V where the maximum EQE was achieved. The half-life time of 500 s under high applied bias of 7 V shows the feasibility for electrically pumped perovskite lasers with further device optimization. These findings suggest the promise of perovskite light-emitting devices under electrical pumping.

Acknowledgments

ORCID iDs

Chen Zou ⬤ https://orcid.org/0000-0001-9638-6363

References

[1] Cho H *et al* 2015 *Science* **350** 1222
[2] Tan Z K *et al* 2014 *Nat. Nanotechnol.* **9** 687
[3] Wang J *et al* 2015 *Adv. Mater.* **27** 2311
[4] Kumawat N K, Dey A, Narasimhan K and Kabra D 2015 *ACS Photonics* **2** 349
[5] Kim Y H, Cho H, Heo J H, Kim T S, Myoung N, Lee C L, Im S H and Lee T W 2015 *Adv. Mater.* **27** 1248
[6] Hoye R L, Chua M R, Musselman K P, Li G, Lai M L, Tan Z K, Greenham N C, MacManus-Driscoll J L, Friend R H and Credgington D 2015 *Adv. Mater.* **27** 1414
[7] Yu J C *et al* 2015 *Adv. Mater.* **27** 3492
[8] Yantara N, Bhaumik S, Yan F, Sabba D, Dewi H A, Mathews N, Boix P P, Demir H V and Mhaisalkar S 2015 *J. Phys. Chem. Lett.* **6** 4360
[9] Ling Y *et al* 2016 *Adv. Mater.* **28** 8983
[10] Swarnkar A, Marshall A R, Sanehira E M, Chernomordik B D, Moore D T, Christians J A, Chakrabarti T and Luther J M 2016 *Science* **354** 92
[11] Li G *et al* 2016 *Adv. Mater.* **28** 3528
[12] Zhang X L, Xu B, Zhang J B, Gao Y, Zheng Y J, Wang K and Sun X W 2016 *Adv. Funct. Mater.* **26** 4595
[13] Zhang X, Xu B, Wang W, Liu S, Zheng Y, Chen S, Wang K and Sun X W 2017 *ACS Appl. Mater. Interfaces* **9** 4926
[14] Zhang X, Lin H, Huang H, Reckmeier C, Zhang Y, Choy W C and Rogach A L 2016 *Nano Lett.* **16** 1415
[15] Wei Z, Perumal A, Su R, Sushant S, Xing J, Zhang Q, Tan S T, Demir H V and Xiong Q 2016 *Nanoscale* **8** 18021
[16] Song J, Li J, Li X, Xu L, Dong Y and Zeng H 2015 *Adv. Mater.* **27** 7162
[17] Chiba T, Hoshi K, Pu Y J, Takeda Y, Hayashi Y, Ohisa S, Kawata S and Kido J 2017 *ACS Appl. Mater. Interfaces* **9** 18054
[18] Davis N J *et al* 2017 *J. Phys. Chem. C* **121** 3790
[19] Yassitepe E, Yang Z, Voznyy O, Kim Y, Walters G, Castañeda J A, Kanjanaboos P, Yuan M, Gong X and Fan F 2016 *Adv. Funct. Mater.* **26** 8757
[20] Li Z, Yang M, Park J-S, Wei S-H, Berry J J and Zhu K 2015 *Chem. Mater.* **28** 284
[21] Liu X, Hong R and Tian C 2009 *J. Mater. Sci., Mater. Electron.* **20** 323
[22] Protesescu L *et al* 2017 *ACS Nano* **11** 3119
[23] Li J *et al* 2017 *Adv. Mater.* **29** 1603885
[24] Yuan M *et al* 2016 *Nat. Nanotechnol.* **11** 872
[25] Rose A 1955 *Phys. Rev.* **97** 1538
[26] Dong Q, Fang Y, Shao Y, Mulligan P, Qiu J, Cao L and Huang J 2015 *Science* **347** 967
[27] Maculan G, Sheikh A D, Abdelhady A L, Saidaminov M I, Haque M A, Murali B, Alarousu E, Mohammed O F, Wu T and Bakr O M 2015 *J. Phys. Chem. Lett.* **6** 3781
[28] Chin X Y, Cortecchia D, Yin J, Bruno A and Soci C 2015 *Nat. Commun.* **6** 7383
[29] Hetsch F, Zhao N, Kershaw S V and Rogach A L 2013 *Mater. Today* **16** 312

[30] Veldhuis S A, Boix P P, Yantara N, Li M, Sum T C, Mathews N and Mhaisalkar S G 2016 *Adv. Mater.* **28** 6804

[31] Stoumpos C C, Malliakas C D and Kanatzidis M G 2013 *Inorg. Chem.* **52** 9019

[32] Sutherland B R and Sargent E H 2016 *Nat. Photon.* **10** 295

[33] Jaramillo-Quintero O A, Sanchez R S, Rincon M and Mora-Sero I 2015 *J. Phys. Chem. Lett.* **6** 1883

[34] Liu X, Li H, Song C, Liao Y and Tian M 2009 *Opt. Lett.* **34** 503

[35] Shi Z, Li Y, Zhang Y, Chen Y, Li X, Wu D, Xu T, Shan C and Du G 2017 *Nano Lett.* **17** 313